ROBUST CONTROL OF FLEXIBLE ROTOR-MAGNETIC BEARING SYSTEMS USING DISCRETE TIME SLIDING MODE CONTROL

Hongqi Tian * and Kenzo Nonami

Chiba University, 1-33 Yayoi-cho, Inage-ku, Chiba 263 Japan

ABSTRACT

This paper is concerned with the computer-based sliding mode control of flexible rotor-magnetic bearing systems (FR-MBS). The plant dynamics consisting of actuator dynamics and flexible rotor dynamics are described. The reduced order model for controller design is given by eliminating higher order modes of the mechanical and electrical magnetic interaction system. A discrete time sliding mode controller, which can alleviate the chattering phenomenon happened in continuous sliding mode system, with reduced order VSS observer is proposed and its robust performances are evaluated with several simulations based on the calculating model.This digital controller is implemented for replacing a linear analog PID compensator. The levitation tests using the proposed digital controller are done and compared with that of the PID compensator. With discrete time sliding mode controller the running test with high speed rotation is successfully increased up to 40000 rpm without unstable vibration.

1. INTRODUCTION

Magnetic bearings are used in high speed rotating machinery with many advantages.The advantages of magnetic bearings applied to support a rotor system are its contactless nature, the capability of high speed rotation and active vibration control. So it is necessary to use an asymptotically stable and robust controller for magnetic bearing to support rotor systems. Now the most controllers designed have been developed by using the linear feedback approaches[1,2]. These control schemes can easily accommodate the cross feedback capability through the utilization of the full-state feedback elements with observers. However, it is not easy to satisfy the robust performance of control systems using linear control low.

* Currently in Seiko Seiki Co., Ltd., Chiba, Japan

For Variable Structure Control System(VSCS), a discontinuous control law is obtained using sliding mode controller which switches when the trajectory crosses certain chosen hyperplane, which is called the sliding manifold, and reaches the origin of state space [3]. Recently some researches have been made for control of rotor-magnetic bearing systems using sliding mode control [4,5]. However, these references did not consider the flexibility of plant and the plant modeling used was simplified and idealized. In recent paper[6,7], the design approach using sliding mode control was extended to the flexible rotor-magnetic bearing systems. However, sliding mode control based on a continuous system is usually implemented using a digital computer. The sampling interval in continuous systems may bring the chattering along the redesigned sliding mode and make the system unstable. Therefore, the discrete time sliding mode controller using a constant sampling should be used for a computer-based control of a practical system[8].

Based on the early works [6,7], this paper describes the design method and the implementation of the discrete time sliding mode controller for an actual flexible rotor-magnetic bearing system. First, the flexible rotor of continuous body based on the test rig is modelled as the discrete mass rotor using a finite element method. The state-space model governing the dynamics of the flexible rotor is described and the reduced order models which includes only the rigid modes is proposed for the design of controller. Then, a new design method of the discrete time sliding mode controller concerning with the external disturbance is presented. Finally, the implementation of this controller is described in comparison of its performance with that of conventional analog compensator.

2. MODELLING OF FR-MBS

The dynamics of the flexible-rotor magnetic bearing system will be described in this chapter. For

simplicity, the analysis is only done in the X direction and all the coupling effects among the different axes and noncollocation are ignored. According to the test rig which will be described in chapter 5, the rotor can be taken simply into account six parts shown in Fig.1.

2.1 Flexible Rotor Dynamics

The discrete model with fourteen order is obtained using finite element method as follows

$$M_0 \ddot{q} + K_0 q = 0 \qquad (1)$$

where

$$q = [x_1 \theta_1 \; x_2 \; \theta_2 \; x_3 \; \theta_3 \; x_4 \; \theta_4 \; x_5 \; \theta_5 \; x_6 \; \theta_6 \; x_7 \; \theta_7 \;]^T$$

and x_i, θ_i $(i=1,\cdots,7)$ represent displacement and angle of the mass on this rotor respectively, especially, x_3 and x_5 represent the positions where the electromagnets are located, M_0 is the mass matrix, K_0 is the stiffness matrix.

2.2 Actuator Dynamics

The attractive force due to an electromagnet can be generally given by

$$P = \frac{A}{\mu_0} B^2 = \frac{A}{\mu_0} \left[\frac{N (i_0 + i)}{\frac{1}{\mu} + \frac{x_0 + x}{\mu_0}} \right]^2 \qquad (2)$$

where P is the attractive force, μ_0 is the permeability in the air, A is the air gap area of one pole, B is the magnetic flux densities, N is the number of winding turns, i_0 is the steady-state current, x_0 is the steady-state gap length, i is the control current, x is the control gap, and μ is the permeability in the magnetic body. Using the Taylor series expansion for small values of i and x, we can get the following attractive force with linear terms

$$P \cong p_0 - k_1 x + k_2 i = p_0 + p \qquad (3)$$

where

$$k_1 = \frac{2 A N^2 i_0^2}{\mu_0^2 (\frac{1}{\mu} + \frac{x_0}{\mu_0})^3} = \frac{2 p_0}{\mu_0 (\frac{1}{\mu} + \frac{x_0}{\mu_0})}$$

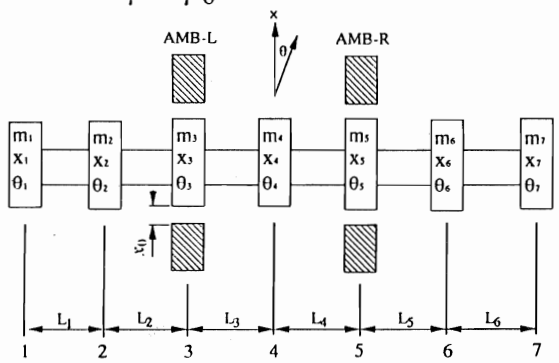

Fig.1 Model of flexible rotor-magnetic bearing system

$$k_2 = \frac{2 A N^2 i_0}{\mu_0 (\frac{1}{\mu} + \frac{x_0}{\mu_0})^2} = \frac{2 p_0}{i_0}$$

and p_0 is the bias attractive force. Considering the pair of attractive forces, the magnetic force P' due to the electromagnet along the radial direction X can be modeled as the following equation:

$$P' = P_1 - P_2 = -2 k_1 x + 2 k_2 i \qquad (4)$$

where P_1 and P_2 are the left and right magnet forces, respectively. Eq.(4) indicates that the actuator total forces on each direction.

2.3 Plant Dynamics

The flexible rotor shown in Fig.1 is restricted by the attractive forces given in Eq.(4). It results

$$M_0 \ddot{q} + K_0 q = F p' + D \qquad (5)$$

where

$$F = \begin{bmatrix} 0 & 0 & 0 & 0 & 1 & 0 & 0 & 0 & 0 & 0 & 0 & 0 & 0 & 0 \\ 0 & 0 & 0 & 0 & 0 & 0 & 0 & 0 & 1 & 0 & 0 & 0 & 0 & 0 \end{bmatrix}^T$$

$$p' = [p_l', p_r']^T$$

$P_l' = 2 k_1 x_3 - 2 k_2 i_l$: forces of the AMB-L

$P_r' = 2 k_1 x_5 - 2 k_2 i_r$: forces of the AMB-R

and D represents the parameter uncertainty and external disturbance.

The bias attractive forces and the control forces of Eq.(5) are separated as follows:

$$M_0 \ddot{q} + K q = F_i i + D \qquad (6)$$

where

$$i = [\, i_l \; i_r]^T \qquad K = K_0 + K_i$$

$$K_i = diag\,(0\,0\,0\,0\;-2k_1\;0\,0\,0\;-2k_1\;0\,0\,0\,0\,0)$$

$$F_i = \begin{bmatrix} 0 & 0 & 0 & 0 & -2k_2 & 0 & 0 & 0 & 0 & 0 & 0 & 0 & 0 & 0 \\ 0 & 0 & 0 & 0 & 0 & 0 & 0 & 0 & -2k_2 & 0 & 0 & 0 & 0 & 0 \end{bmatrix}^T$$

Using the modal analysis technique, we can choose the following normalized modal matrix,

$$q = \Psi \xi \qquad (7)$$

Equation (6) is transformed to the form in model coordinate as follows:

$$\ddot{\xi} + \Lambda \dot{\xi} + \Omega^2 \xi = f_i i + d \qquad (8)$$

where

$$I = \Psi^T M \Psi \qquad \Omega^2 = \Psi^T K \Psi \qquad \Lambda = 2 \zeta \Omega$$

$$f_i = \Psi^T F_i \qquad d = \Psi^T D$$

where Λ is called the damping matrix. The damping ratio is determined experimentally. The state equation of the electromagnetic-mechanical system is given by

$$\dot{x}_f = A_f x_f + B_f u + D_f \qquad (9)$$

where

$$x_f = \begin{bmatrix} \xi & \dot{\xi} \end{bmatrix}^T \qquad u = \begin{bmatrix} i_l & i_r \end{bmatrix}^T$$

$$A_f = \begin{bmatrix} 0 & I \\ -\Omega^2 & -\Lambda \end{bmatrix} \quad B_f = \begin{bmatrix} 0 \\ f_i \end{bmatrix} \quad D_f = \begin{bmatrix} 0 \\ d \end{bmatrix}$$

If the rotor displacement at the magnetic bearings can be measured, the output equation is

$$y = C_f x_f = \begin{bmatrix} x_3 & x_5 \end{bmatrix}^T \tag{10}$$

where

$$C_f = \begin{bmatrix} F_i^T \Psi & 0 \end{bmatrix}$$

2.4 Reduced Order Model

Because this MIMO system is originally unstable in open loop, the control objective is to levitate the rotor and maintain the stability. In this case, there are only two unstable rigid modes, and the flexible modes are essentially stable. It is complicated to design a controller including full order models for this high order flexible system. Therefore, the construction of the reduced order model is considered upon the standpoint to stabilize the two rigid modes and to control the vibration of flexible modes. The reduced order model is constructed by truncation of the higher order modes in modal coordinates. Here, the state equation and the output equation including till the *ith* order mode are written as follows:

$$\dot{x}_r = A_r x_r + B_r u + D_r$$
$$y = C_r x_r = \begin{bmatrix} x_3 & x_5 \end{bmatrix}^T \tag{11}$$

where

$$x_r = \begin{bmatrix} \xi_1, \xi_2, \cdots, \xi_i; \dot{\xi}_1, \dot{\xi}_2, \cdots, \dot{\xi}_i \end{bmatrix}^T$$

Concerning the reduced order model of Eq.(11), the design of control system are done with the case which only the rigid modes are considered. In addition, the closed loop system has to maintain the robust stability without spillover caused by higher order modes ignored above.

3. DISCRETE TIME SLIDING MODE CONTROLLER OF FR-MBS

As limitation of the structure, this magnetic bearing system has only two output feedbacks which may be measured directly. Therefore, a robust variable structure system (VSS) observers designed in Ref.[6] is used for system state estimation. Considering the reduced order model system given in Eq.(11), the equivalent discrete-time system is found as

$$x_r(k+1) = \Phi x_r(k) + \Gamma u(k) + d(k)$$
$$\begin{bmatrix} y(k) \\ z(k) \end{bmatrix} = \begin{bmatrix} C_r \\ C_p \end{bmatrix} x_r(k) \tag{12}$$

where

$$\Phi = exp(A_r \Delta)$$
$$\Gamma = A_r^{-1} [\, exp(A_r \Delta) - I \,] B_r$$

Δ is the sampling time, z is estimated state variables with VSS observer and $C_p \in R^{(n-l)\times n}$.

In this discrete time system, the following matching condition is guaranteed.

$$d(k) = \Gamma f(k) \tag{13}$$

where

$$|f(k)| \le F_{max}$$

and F_{max} is the estimated maximum values of external disturbance.

The sliding manifold is defined by

$$\sigma(k) = S x_r(k) \tag{14}$$

After the system state is driven into the sliding mode at the time of $k_i \Delta$, using the condition of $\sigma(k) = \sigma(k+1)$ $(k > k_i)$, the equivalent control in the sliding mode can be got as

$$u_{eq}(k) = L x_r(k) \tag{15}$$

where

$$L = -(S\Gamma)^{-1} S (\Phi - I)$$

The ideal sliding motion is then described by the system equation

$$x_r(k+1) = [\Phi - \Gamma (S\Gamma)^{-1} S (\Phi - I)] x_r(k) \tag{16}$$
$$S x_r(k) = 0$$

3.1 Selection of Switching Manifolds

In the first step, S must be determined for a given set of stable G, that means the eigenvalues of Eq.(16) must be lie within the unit circle. Considering the reduced order system shown in Eq.(12), where $rank(B_r)=m = 2$ and $n=4$. the system equation can be changed into following form

$$x_r^1(k+1) = \Phi_{11} x_r^1(k) + \Phi_{12} x_r^2(k) \tag{17}$$
$$x_r^2(k+1) = \Phi_{21} x_r^1(k) + \Phi_{22} x_r^2(k) + \Gamma_2 u(k) + \Gamma_2 f(k) \tag{18}$$

where

$$\Phi = \begin{bmatrix} \Phi_{11} & \Phi_{12} \\ \Phi_{21} & \Phi_{22} \end{bmatrix}, \qquad \Gamma = \begin{bmatrix} 0 \\ \Gamma_2 \end{bmatrix}$$

$x_r^1 \in R^{n-m}$, $x_r^2 \in R^m$, Γ_2 is $m \times m$ nonsingular matrix and Φ_{11} is (n-m)×(n-m) matrix. For the switching hyperplane defined in Eq.(14), it is transformed to

$$\sigma(k) = S x_r(k) = S_1 x_r^1(k) + S_2 x_r^2(k) \tag{19}$$

where S_2 is a non-singular $m \times m$ matrix. Assuming the system is in the sliding mode, Eq.(19) yields

$$x_r^2(k) = -S_2^{-1} S_1 x_r^1(k) = F x_r^1(k) \tag{20}$$

so that the evolution of x_r^2 in the sliding mode is related linearly to that of x_r^1. The sliding mode is governed by Eq.(17) and Eq.(20). This is an $(n-m)$th order system in which x_r^2 holds the role of a full-state feedback control system. Closing the loop in Eq.(17)

with the feedback from Eq.(20)

$$x_r^1(k+1) = (\Phi_{11} + \Phi_{12} F)\, x_r^1(k) \quad (21)$$

so that the design of a stable sliding mode ensuring $x_r \to 0$ as $t \to \infty$ requires to choose the $(n\text{-}m)$ closed-loop eigenvalues of Eq.(21) to lie within the unit circle. These eigenvalues correspond to the $(n\text{-}m)$ non-zero eigenvalues of the equivalent system. The process can be achieved by using a modified form of any standard design method giving a linear feedback controller for a linear dynamical system. The method which is considered in this paper is that based on the minimization of an integral cost functional with quadratic integrand which was discussed in Ref. [6].

3.2 Design of Controller

After the design of switching surface, the next important aspect of variable structure system is guaranteeing the existence of sliding mode. The variable structure system can be thought of as a closed-loop system with an adaptively varying state feedback gain. Therefore, the type of control law considered here consists of two independent functions: a linear state feedback control function u_L and non-linear control function u_{NL}:

$$u(k) = u_L(k) + u_{NL}(k) \quad (22)$$

where

$$u_L(k) = L\, x_r(k)$$

and L is given in Eq.(15). u_{NL} is discontinuous control law which can be defined by

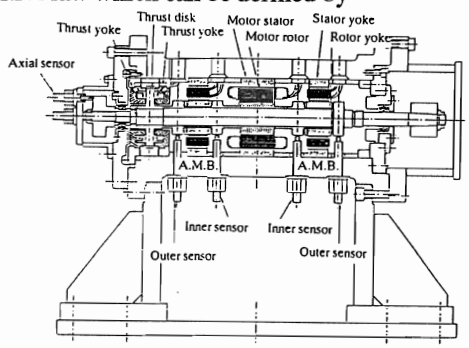

Fig.2 Testing apparatus of magnetic bearing

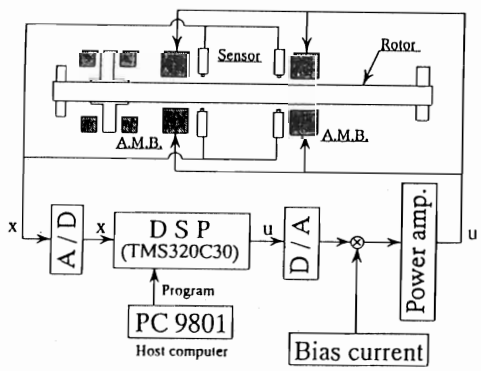

Fig.3 Experimental setup for digital control

$$u_{NL} = -[\alpha(k) + \beta(k)]\, sgn(\sigma(k)) \quad (23)$$

where

$$\alpha(k) = \eta \frac{\|\sigma(k)\|}{\|S\Gamma\|} \quad 0 < \eta < 2,\ \beta(k) \geq F_{max}$$

It can be proved that the control law selected here guarantees the existence condition of sliding mode.

4. EXPERIMENTAL RESULTS

The test rig of the magnetic bearing system under consideration is shown in Fig.2. A induction motor rotor is located in the middle of the shaft and two radial magnetic bearings are located on both sides of the motor rotor. A thrust magnetic bearing is located at left end of the shaft. The radial magnetic bearings together control two rotational and two translational degrees of freedom. The thrust magnetic bearing controls the displacement in the axial direction. Eddy current type proximity sensors are set up for the radial magnetic bearings at both sides of the bearings, but inner sensors are used in tests. The natural frequencies of the first two bending modes measured in an impulse experiment were determined to be 340 Hz and 780 Hz, respectively.

The block diagram of the control system implemented digitally is shown in Fig.3. A digital signal processor $TMS320C30$ with the high-speed A/D converter and D/A converter is used to accomplish digital control and to transfer of data between the a host personal computer and test rig. The sampling time in experiments is selected to 0.4 ms because it is not necessary to take a small sampling rate like continuous system. In fact, the computation time for the control algorithm was less than 0.1 ms. Therefore, the proposed discrete time sliding mode controller is expanded to control two directions (x *and* y) simultaneously. Other controller parameters are the same as those used for simulations.

In this experimental set up, a linear analog compensator was also applied in each axis based on the models ignoring the coupling effects among various axes. we can choose the control system by either the linear analog compensator, or the discrete time sliding mode controller designed.The compensator circuit is made up of an integration circuit to increase static rigidity, a phase lead circuit to increase the damping force of the rotor in the intermediate frequency range and a low pass filter to attenuate the gain in high frequency range.

Figure 4 shows the typical time history response of the discrete time sliding mode control system at the lift off. The time history response of the analog compensator in same position is presented in Fig.5. The time history response of the sliding mode

controller shows that it takes about 80 *ms* to reach the steady-state position whereas the analog controller

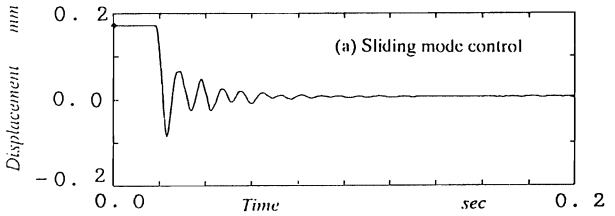

Fig.4 Time history responses of digital controller

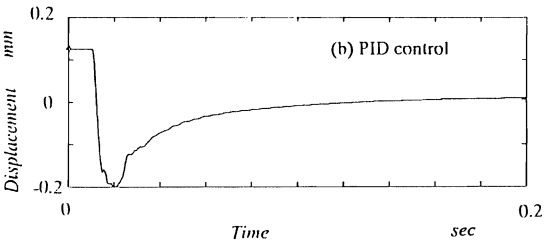

Fig.5 Time history responses of analog compensator

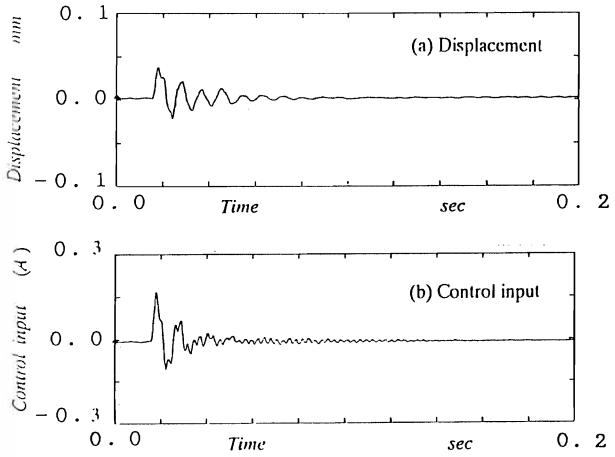

Fig.6 Impulse response of digital controller

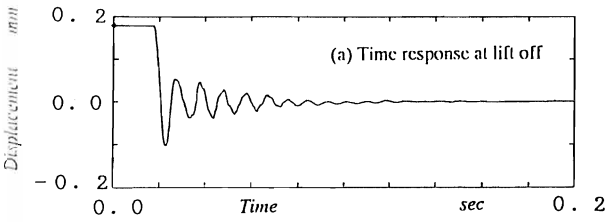

Fig.7 Time history responses of digital controller

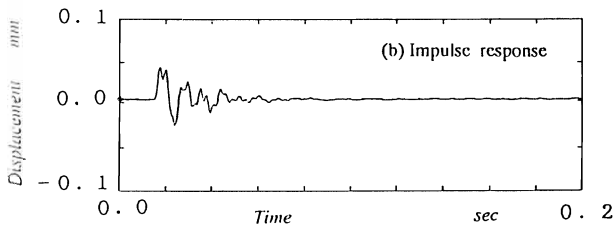

Fig.8 Impulse response of digital controller

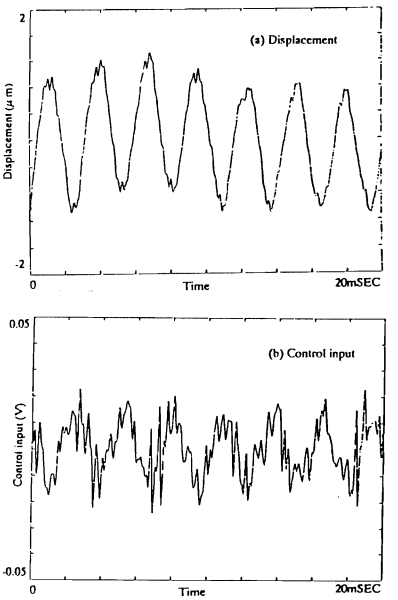

Fig.9 Waveform of x-direction in rotation (20,000rpm).

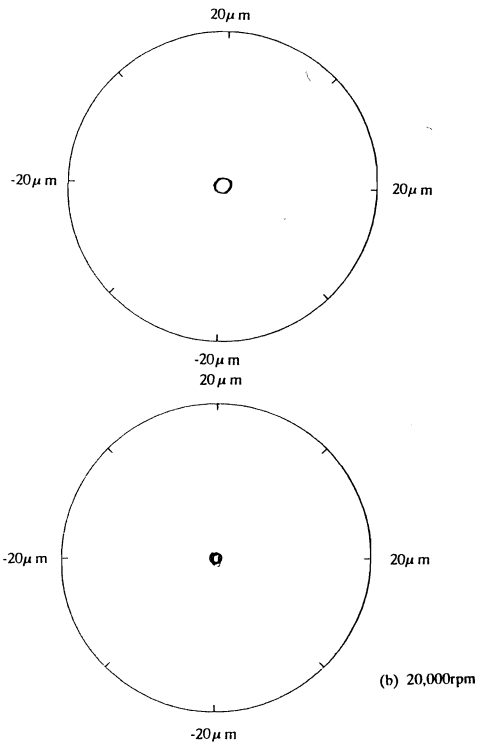

Fig.10 Orbit plot of shaft centre at position x_3

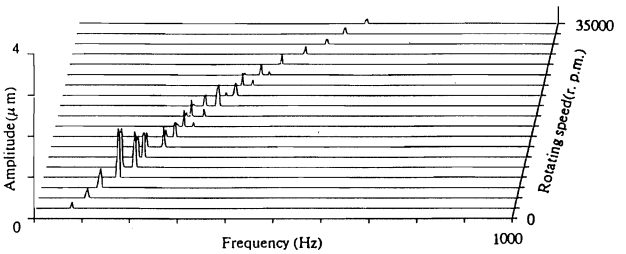

Fig.11 Waterfall diagram of shaft vibration in x-direction

takes over 200 *ms* with a big overshoot. Figure 6 gives the impulse responses of the sliding mode control when the disturbance is added at the right end of the rotor. This impulse response indicates an excellent performance considering that the controller was designed using only rigid mode. The control current to realize this response is also shown in that same figure. It can be also found that the experimental data have good agreement with the simulation results. Considering the robustness of sliding mode controller, Figure 7 and Figure 8 show respectively the time history responses and the impulse response in the case of the increment of the rotor mass to 50% of the nominal value by loading a mass at the right end of rotor. It can be seen that the system is still stable to be suspended and the discrete time sliding mode controller designed has superior performances to eliminate disturbances and to maintain the low sensitivity for the system parameter variation. It is not easy for conventional analog compensator to realize the similar good performance.

Next, we would give the results of rotating test with sliding mode controller for this test rig. Figure 9 shows the waveform of control current and shaft vibration of x-direction at first bending critical speed(20,000rpm). In this figure, the control current made by discrete time sliding mode controller has the same period as the shaft vibration. We can also find the shaft vibration has the very small magnitude though the shaft is rotated under first bending mode. For showing the shaft vibration of xy-direction in same time, Figure 10 gives the orbit plot of shaft centre at position x_3 under rigid mode(8,000rpm) and first bending mode(20,000rpm). It is shown from this figure that the vibration magnitude in rigid mode is larger than that of first bending mode, but the spillover phenomena, which is caused by ignored higher order modes, can not be found in both cases. Finally, a waterfall diagram of shaft vibration in the rotation test is attained as shown in Fig. 11. With discrete time sliding mode controller the rotating test was successfully rotated up to 40000 rpm without unstable vibration in this case. As the result the vibration frequency of shaft is proportional to the rotating speed in whole frequency ranges, and the vibration response is fully damped even at the rigid and first bending critical speed.

5. CONCLUSIONS

This paper have developed the active vibration control system for the actual flexible rotor-magnetic bearing systems by considering the instability, nonlinearity and flexibility of the plant. Using finite element method, the state space model for the full order system of the flexible rotor is derived. The plant dynamics including the actuator dynamics and the flexible rotor are described. The discrete time sliding mode controller using the reduced order model of plant, which can control effectively the full order system with robustness to the spillover phenomena of the higher order modes, have been designed for active control of magnetic bearing systems. The new discrete time VSS observer and the simple algorithm for digital controller design are proposed. It is have shown that this controller can alleviate the chattering phenomenon happened in continuous sliding mode system. This controller is implemented as an alternative to a conventional linear analog PID compensator. The comparisons between results of the discrete time sliding mode controller and the analog PID compensator, which is carried out in levitation tests, indicated that the digital controller has superior dynamic response properties and robustness for the system parameter uncertainty, nonlinear factors and external disturbances.With discrete time sliding mode controller the rotating test is successfully increased up to 40000 rpm without unstable vibration like chattering, which indicated that the vibration responses are fully damped even at the rigid and first bending critical speed.

ACKNOWLEDGMENTS

The authors gratefully acknowledge the support of Ebara Research Co., Ltd. of Japan for the experimental set up.

REFERENCES

[1] E.H.Maslen and J.R.Bielk, Transactions of ASME, Journal of Dynamic Systems, Measurement, and Control, 114, (1992), p.172.

[2] C.D.Bradfield, J.B.Roberts and S.Karunendiran, Transactions of ASME, Journal of Vibration and Acoustics, 113, (1991), p.160.

[3] K.Nonami and H. Tian: Sliding Mode Control, Korona Publ., Japan, [1994].

[4] K.Nonami and H.Yamaguchi, Transactions of JSME (in Japanese), C, 58, (1991), p.106.

[5] A.Sinha, K.L.Mease and K.W.Wang, ASME Biennial Conference on Mechanical Vibration and Noise, Miami, Florida, U.S.A., (1991), p.209.

[6] H. Tian and K.Nonami, Int.Conf. on Advanced Mechatronics, Tokyo, Japan, (1993), p.475.

[7] H.Tian, K. Nonami and M. Kubota, Asia-Pacific Vibration Conference '93, Japan, (1993), p.987.

[8] K.Furuta, System & Control Letters,14, (1990), p.145.